Density effects on salt tracer breakthrough curves from constructed wetland ponds

Bernhard H. Schmid[1], Michael A. Hengl[2] and Ursula Stephan[2]

[1]Institut für Hydraulik, Gewässerkunde und Wasserwirtschaft, Technische Universität Wien, c/o Vegagasse 16, A-1190 Vienna, Austria

[2]Institut für Wasserbau und hydrometrische Prüfung, Bundesamt für Wasserwirtschaft, A-1090 Vienna, Austria

E-mail: *schmid@hydro.tuwien.ac.at*

Received 16 August 2002; accepted in revised form 28 January 2004

Abstract Salt tracer experiments are a convenient method to determine travel time distributions in constructed wetland ponds. Typically, these flows are characterized by low Reynolds numbers at times even within the laminar flow regime. In this environment the injection of salt may cause strong density effects, thereby jeopardizing the usefulness of the recorded breakthrough curves. After a tracer experiment has been completed, an indication of potential density stratification in the field may be noticed in the form of surprisingly small recovery rates of a tracer considered as nearly conservative.

To provide a tool that permits the intended experiment to be judged at the planning stage already, criteria have been developed that yield approximate maximum concentrations, not to be exceeded if density effects shall be avoided. Laboratory experiments were carried out and the newly derived relationships applied with success. The criteria may in future be useful, too, in the planning of tracer experiments in slowly flowing rivers and streams.

Keywords Constructed wetlands; density effects; solute transport; stratification; tracers

Nordic Hydrology **Vol 35 No 3 pp 237–250** © IWA Publishing 2004

Notation

B width (m)
B_i integration constant (B_s for smooth and B_r for rough beds)
C concentration (mg/l)
C_0 initial concentration (mg/l)
$C_{\max}$ highest initial salt concentration without strong density effects (mg/l)
Fr Froude number (-)
$Fr*$ Froude number, computed from shear velocity $Fr* = u*/\sqrt{gh}$
g acceleration of gravity (m/s^2)
h water depth (m)
k_s bed roughness (m)
M_0 mass of salt injected (g)
q discharge per unit width (m^2/s)
Q flow rate (m^3/s)
Re Reynolds number (−)
R_h hydraulic radius (m)
Ri Richardson number (−)
Ri_b bulk Richardson number (−)
S friction slope (−)
T temperature (°C)
u velocity component in streamwise direction (m/s)
$\bar{u}$ mean flow velocity (m/s)
$u*$ shear velocity (m/s)

z vertical coordinate (m), positive upwards
δ height above bottom (m) of the point of maximum velocity
Δt duration of pulse injection (s)
κ Karman's constant $(-) \approx 0.4$
ν kinematic viscosity (m^2/s)
Π Cole's wake parameter $(-)$
ρ fluid density (kg/l)
τ shear stress (N/m^2)

Introduction

Especially in the Nordic countries the importance of local wastewater treatment has been increasing strongly over the past two decades. Since 1985, constructed wetlands have been among the most rapidly expanding wastewater treatment systems (Kadlec and Knight 1996). In terms of their hydraulic characteristics, the following kinds of constructed wetlands can be distinguished: the free water surface (FWS) type with or without vegetation, the groundwater flow (GWF) type with a porous media passage and the combined overland and groundwater flow (OGF) type. It is the first of these three types mentioned (wetland ponds, without vegetation) that will be addressed here.

The removal efficiency and effectiveness of wetland ponds is strongly related to the distribution of flow paths, the ideal being plug flow conditions in the pond (Persson *et al.* 1999). This distribution of flow paths is, in turn, reflected by concentration–time distributions or breakthrough curves of an ideal tracer injected into the flow (near-instantaneous slug release or relatively short pulse injection). It is not surprising, therefore, that tracer experiments are frequently used to study particle travel time distributions and flow paths, thereby hoping to obtain indications of hydraulic and removal efficiency. Tracers available range from various salts (e.g. KBr) to dyes (such as Rhodamin WT) to radioactive substances (primarily tritium oxide) and, most recently, artificially produced pieces of DNA chains (Sabir *et al.* 2000). The tracers most commonly used in wetland studies are salts and tritium, with tritium injections being not generally applicable due to a restrictive permissions policy in some European countries. Users of salt tracers, however, run the risk of having their results compromised by density effects, especially in cases of slow to near-stagnant flows at particularly low Reynolds numbers, and it is just this type of near-laminar or only weakly turbulent flows that is often encountered in wetlands (e.g. Hammer and Kadlec 1986). It is the purpose of this paper to present a method that permits the risk of compromising density effects to be estimated already at the planning stage of an intended salt tracer experiment.

Theory

The importance of vertical exchange processes and, thus, the presence of density stratification, can be characterized by a non-dimensional number, the Richardson number (see, for example, Rutherford (1994)), defined by

$$Ri = -\frac{g}{\rho}\frac{\partial\rho/\partial z}{(\partial u/\partial z)^2} \tag{1}$$

with

ρ = density of the fluid,
g = acceleration of gravity,
z = vertical coordinate (positive upwards) and
u = velocity component in streamwise direction.

This number measures the relative importance of two counteracting influences: the density gradient, favouring the development of a stable layer, and the mixing action of shear due to

a gradient in streamwise velocity. Miles (1962) and Howard (1962) showed that a shear flow can become unstable as the gradient Richardson number decreases below 0.25. Following a different argument the same result was obtained and, thus, confirmed by Boehrer *et al.* (2000). Rutherford (1994) distinguished between fast flowing rivers with, typically, $Ri < 1$ and stratified flows with $5 < Ri < 10$. Strongly stratified flows with $Ri > 10$ are described as having a sharp interface, with vertical mixing being largely due to instabilities in internal waves rather than eddy diffusion. Using the values of velocity and density at the water surface and the channel bottom only, a bulk Richardson number can be introduced:

$$Ri_{\mathrm{b}} = -\frac{g}{\rho}\frac{\Delta\rho/\Delta z}{(\Delta u/\Delta z)^2} = -\frac{gh}{\rho}\frac{\Delta\rho}{(\Delta u)^2} \tag{2}$$

with h denoting water depth and Δ a difference between surface and bottom values. In Eq. (2), ρ is the depth-averaged density (Rutherford 1994), but in weakly stratified flows surface or bottom values can be used, if convenient, without introducing significant errors.

Values of the bulk Richardson number exceeding unity are associated with stable stratification, whereas for $Ri_{\mathrm{b}} < 0.25$ buoyancy effects remain small (Rutherford 1994), which essentially agrees with the above-mentioned results by Miles (1962), Howard (1962) and Boehrer *et al.* (2000). Consequently, a criterion of negligible density effects can be given as

$$Ri_b \leq 0.25 \tag{3}$$

which is as straightforward as it is impractical from the viewpoint of tracer experiment design, as the bulk Richardson number is unknown *a priori*. To overcome this difficulty, $\Delta\rho/\rho$ and Δu must be estimated.

The density difference $\Delta\rho$ of interest here is entirely due to the salt concentration. Subsequently, it will be assumed that the tracer becomes vertically fully mixed right after the release (e.g. by injection into a sufficiently strong inflow weir overfall). The maximum concentration in a vertical profile in the wetland pond can therefore be approximated by

$$C_{\max} = \frac{M_0}{Q\Delta t} \tag{4}$$

with M_0 as the salt tracer mass [g] injected, Q is the discharge [m^3/s] and Δt is the duration of the injection pulse (s), which yields g/m^3 or mg/l as the units of concentration.

After the tracer release has stopped, the inflow again consists of water without added tracer, so that $C = 0$ (the background, if any, has been subtracted here). During the salt tracer release, a near-constant vertical concentration profile close to the inflow cross section of the wetland pond can be assumed due to full vertical mixing, with concentration close to the value given by Eq. (4). After the release has stopped, the current will move fresh inflow water (without added tracer now, i.e. $C = 0$) over the salt-enriched water lower down in the profile, as the streamwise flow velocities increase with distance from the bottom. It may be added that the so-called velocity dip (the highest velocity not at the surface, but at a point lower down) is assumed to be absent here, which is mostly correct, if (and this is usually quite realistic) the wetland pond cross section is wide (aspect ratio $B/h > 5$ for turbulent flows, see Nezu *et al.* (1993)). Thus, in our approximate model of the density stratification, we have a concentration of $C = 0$ at the surface and $C = C_{\max}$ (Eq. (4)) at the bottom. What is needed now is a relationship that links the concentration difference to the associated density difference required to evaluate the bulk Richardson number. In the temperature and concentration ranges of interest here, the formula proposed by Crowley (1968) can be applied with success:

$$\rho(T, C) = 1 + 10^{-3}[28.14 - 0.0735T - 0.00469T^2 + (0.802 - 0.002T)(C - 35)] \tag{5}$$

with density ρ [kg/l], temperature T [°C] and salinity C [ppt] $\approx$ salt concentration $C[g/l] = 10^{-3}C$ [mg/l] for the dilute solutions treated here. A change in ρ due to a change in salt concentration of $\Delta C = C(z = h) - C(z = 0) = -C_{\max}$ [mg/l] then becomes

$$\Delta\rho \approx -10^{-6}(0.802 - 0.002T)C_{\max}. \tag{6}$$

Whereas the differences in the respective densities of the surface and bottom water are of importance here, as they may or may not give rise to a stable stratification, the absolute value of ρ in the denominator of $\Delta\rho/\rho$ still differs only little from unity, so that we can write

$$\frac{\Delta\rho}{\rho} \approx -10^{-6}(0.802 - 0.002T)C_{\max} \tag{7}$$

which expresses the previously unknown density term in the Richardson number with the aid of a known concentration (Eq. (4)).

While the background to the Crowley (1968) formula is physical oceanography (so that "salinity" must be taken to mean primarily NaCl), checks performed by the authors have shown the relationship to work quite well with other salts like KBr too. So, for instance, measurements of KBr solution density with salt concentrations of $C = 0$ g/l and $C = 3.945$ g/l at different temperatures (20°C and 30°C, respectively) gave density differences of 0.0029 kg/l at either temperature, with the Crowley formula, Eq. (5), predicting 0.0030 kg/l, which is just 0.0001 kg/l more. Compared to tabulated values of the density of pure water, Eq. (5) produces a relative error of less than 0.03% in the range between 0°C and 35°C. Relative changes of density with temperature, however, are not reproduced well below 10°C and the relationship does not show a maximum pure water density at 4°C. This, however, has no effect on the work presented here, as density differences only due to differences in salt concentrations are considered.

Now only the term Δu remains to be treated and this derivation will depend on the (vertical) velocity distribution. The velocity distribution is, in turn, a function of the flow regime, i.e. primarily laminar, turbulent (smooth) or turbulent (rough).

Although the laminar regime as such is quite rare in open channel flows, the near-stagnant conditions frequently encountered in wetland ponds may well qualify for it. A usual Reynolds number criterion is (see, for example, Rutherford 1994)

$$Re = \frac{\bar{u}h}{\nu} < 500 \quad \text{(laminar)} \tag{8}$$

and

$$Re > 2000 \ \text{(turbulent)} \tag{9}$$

with a transition between 500 and 2000. $\bar{u}$ denotes mean flow velocity, h is water depth and ν is kinematic viscosity.

For laminar flows, the velocity distribution is parabolic and can be written as

$$u(z) = \frac{24gS}{K\nu} z\left(h - \frac{z}{2}\right) \tag{10}$$

with S the friction slope and K a roughness parameter ($K = 24$ for a smooth surface; otherwise values can be taken from, for example, Woolhiser (1975)).

The velocity difference $\Delta u = u(z = h) - u(z = 0) = u(z = h)$ so that, from Eq. (10), one has

$$\Delta u = \frac{12gh^2}{\nu}\frac{S}{K}. \tag{11}$$

Integration of $u(z)$, Eq. (10), over the water depth yields the discharge q per unit width and the depth-averaged streamwise flow velocity $\bar{u}$ (known or at least easily measurable quantities):

$$q = \bar{u}h = \frac{8gh^3}{\nu}\frac{S}{K} \tag{12}$$

which permits S/K of Eq. (11) to be replaced by an expression containing q (or $\bar{u}$), g, h and ν, thereby avoiding the need to determine S and K in the field (which, due to the flat water surface in the wetland pond, may be difficult to achieve reliably). Thus, we obtain

$$(\Delta u)^2 = \frac{9}{4}\frac{q^2}{h^2} = \frac{9}{4}(\bar{u})^2. \tag{13}$$

Substitution of Eqs. (7) and (13) into Eq. (2) finally yields, after rearrangement,

$$C_{\max}[\mathrm{mg/l}] = \frac{562500}{0.802 - 0.002T[^\circ\mathrm{C}]}Fr^2 \tag{14}$$

as the criterion for the laminar flow case, with $Ri_{\mathrm{b,max}} = 0.25$ and $Fr = \bar{u}/\sqrt{gh}$. For temperatures of 10°C ± 5°C Eq. (14) can be further simplified to

$$C_{\max}[\mathrm{mg/l}] = K_0 Fr^2 \tag{15}$$

with coefficient $K_0 \approx 719300$.

An alternative approach may be followed by using depth averages of $(-1)(1/\rho)(\partial\rho/\partial z)$ and $(\partial u/\partial x)^2$ instead of local values in Eq. (1):

$$\frac{1}{h}\int_0^h (-1)\frac{1}{\rho}\cdot\frac{\partial\rho}{\partial z}\mathrm{d}z = \frac{1}{h}\ln\left[\frac{\rho(z=0)}{\rho(z=h)}\right] \tag{16a}$$

and

$$\frac{1}{h}\int_0^h \left(\frac{\partial u}{\partial z}\right)^2 \mathrm{d}z = \frac{1}{h}\int_0^h \left[\frac{24gS}{K\nu}(h-z)\right]^2 \mathrm{d}z = 3\frac{q^2}{h^4} \tag{16b}$$

so that

$$\frac{\rho(0)}{\rho(h)} = 1 + \frac{\Delta\rho}{\rho(h)} = \exp\left(\frac{3q^2 Ri_{\max}}{gh^3}\right) = \exp\left(3Fr^2 Ri_{\max}\right) \tag{17}$$

and finally, using Eq. (7) for the density term again:

$$C_{\max}[\mathrm{mg/l}] = \frac{10^6}{0.802 - 0.002T[^\circ\mathrm{C}]}\left[\exp\left(3Fr^2 Ri_{\max}\right) - 1\right]. \tag{18}$$

The use of averages makes the definition of the limiting Richardson number formally different from Eq. (2), which is why the symbol $Ri_{\max}$ is used in Eqs. (17) and (18) rather than $Ri_{\mathrm{b,max}}$ as before. Provided the upper limit $Ri_{\max}$ is taken to be the same as before $Ri_{\mathrm{b,max}}$ (i.e. 0.25), this approach yields a criterion slightly less cautious than Eq. (14), as can be seen from the first-order approximation to the exponential term in Eq. (18), the introduction of which yields, after rearrangement,

$$C_{\max}[\mathrm{mg/l}] = \frac{750000}{0.802 - 0.002T[^\circ\mathrm{C}]}Fr^2. \tag{19}$$

This differs from Eq. (14) by a factor of $3/(9/4) = 1.33$, i.e. Eq. (14) predicts an upper concentration limit that is 75% of the one predicted by Eq. (19). This will be discussed with reference to the experimental data in the following section of this paper.

For turbulent flows the velocity distribution can be described by a form of the log law or by Coles' law including a wake term for the outer region of the flow. In either case, a distinction between a smooth and rough bottom must be made (see, for example, Graf and Cellino (2002)):

$$\frac{u}{u^*} = \frac{1}{\kappa}\ln\left(\frac{z}{L_0}\right) + B_i + \frac{2\Pi}{\kappa}\sin^2\left(\frac{\pi z}{2\delta}\right) \tag{20}$$

with u^* denoting shear velocity, κ is Karman's constant (≈ 0.4), B_i is the integration constant, Π is Coles' wake strength and δ is the height of the point of maximum velocity (here, the surface, therefore $\delta = h$). Subsequently, k_s will be used for the bed roughness.

If the bed is hydraulically smooth, $u^*k_s/\nu < 5$, we have

$$L_0 = \frac{\nu}{u^*} \quad \text{and} \quad B_i = B_s = 5.5 \tag{21}$$

whereas for a hydraulically rough bed, $u^*k_s/\nu > 70$:

$$L_0 = k_s \quad \text{and} \quad B_i = B_r = 8.5 \tag{22}$$

with ν the kinematic viscosity of water (of order of magnitude $10^{-6}\,\mathrm{m^2/s}$: the precise value depends on temperature: at 10°C it is $1.31 \times 10^{-6}\,\mathrm{m^2/s}$, while at 20°C it is $1.01 \times 10^{-6}\,\mathrm{m^2/s}$).

For turbulent flows at comparatively low Reynolds numbers (of up to some 10^4), Nezu and Rodi (1986) stated that the wake strength Π is near zero and this is in agreement with the findings reported here later.

Whereas the density term is still represented by Eq. (7), $(\Delta u)^2$ now becomes

$$(\Delta u)^2 = u^{*2}\left[\frac{1}{\kappa}\ln\left(\frac{h}{L_0}\right) + B_i + \frac{2\Pi}{\kappa}\right]^2 \tag{23}$$

which, substituted together with Eq. (7) into Eq. (2), yields after rearrangement

$$C_{\max}[\mathrm{mg/l}] = \frac{10^6}{0.802 - 0.002T[^\circ\mathrm{C}]}\frac{Ri_{\mathrm{b,max}}Fr^{*2}}{\kappa^2}\left[\ln\left(\frac{h}{L_0}\right) + \kappa B_i + 2\Pi\right]^2 \tag{24}$$

with $Fr^* = u^*/\sqrt{gh}$. Mathematically, the alternative approach of using depth averages of $(-1)(1/\rho)(\partial\rho/\partial z)$ and $(\partial u/\partial z)^2$ is also feasible here but, due to the logarithm, the mean behaviour of $(\partial u/\partial z)^2$ is strongly dominated by the domain near $z = 0$ with a singularity of the function. Formally, the singularity can be avoided by integrating only over the domain of non-negative velocities, but the dominance of the near-bottom region remains and too large values of the mean $(\partial u/\partial z)^2$ result, giving rise to an "unsafe" criterion. This is, consequently, not reproduced here.

A practical problem may arise with respect to the quantification of the shear velocity, u^*, which is needed to evaluate the above criterion, Eq. (24). In open channel flow u^* can usually be readily determined from (see, for example, Henderson (1966))

$$u^* = \sqrt{\frac{\tau}{\rho}} = \sqrt{gR_hS} \approx \sqrt{ghS} \tag{25}$$

with τ the shear stress and R_h the hydraulic radius. In a wetland pond, the slope is frequently too small to be determined accurately. What will, however, be known or can be measured is the inflow to the wetland pond, and so will the width and the depth. Thus, the cross-sectionally averaged flow velocity $\bar{u}$ can be considered as an available quantity in this context. Integrating the flow velocity, Eq. (20), over the depth (and assuming the domain of

theoretically negative velocities to be small), one obtains the following relationship:

$$\frac{\bar{u}}{u^*} = \frac{1}{\kappa}\left[\ln\left(\frac{h}{L_0}\right) - 1\right] + B_i + \frac{\Pi}{\kappa} \tag{26}$$

from which u^* can be computed, once $\bar{u}$ is known (and, in the hydraulically rough case, k_s has been estimated). Note that, for smooth beds, u^* forms part of L_0 and the above relationship becomes implicit (to be solved, for example, iteratively or with the aid of some spreadsheet software).

Experiments and comparison

The formation of salt-induced density stratification was studied experimentally in a 1.5 m wide and some 40 m long, straight, recirculating laboratory flume of rectangular cross section. A previous preliminary study of the hydraulic characteristics of 12 constructed wetland ponds distributed over Norway, Finland, Sweden and Poland had indicated that low Reynolds number flows are quite common in these wetlands. Reynolds numbers at the maximum registered flow rates were of the order of 10^3 in the majority of these 12 cases, with only 1 out of 12 exceeding 10^4. This finding agrees well with the picture of low Reynolds number flows in constructed wetland ponds found in the literature (e.g. Hammer and Kadlec 1986;Kadlec and Knight 1996). Consequently, the majority of the experiments reported here, i.e. 9 out of 14, were conducted at Reynolds numbers around or below 1000, with the other five placed well within the turbulent regime ($Re > 4000$, and thus distinctly above the threshold of some 2000). The water depth was selected as $h \approx 20$ cm for most of the runs, with h $\approx$ 10 cm for the others.

The laboratory set-up described here cannot, of course, fully reproduce conditions in real world constructed wetlands, but it was attempted to choose parameter values relevant to the situation in the field. Reasons for the choice of Reynolds numbers have been given above, and the water depths selected reflect the fact that many wetland ponds have large shallow parts, as in, for example, the free water surface wetlands at Hovi and at Alastaro, Finland (Koskiaho 2003).

Velocities were measured by means of a 3D acoustic doppler velocimeter (ADV) operating at 10 MHz acoustic frequency. The specifications name a velocity resolution of 0.1 mm/s, and the velocity range was set to ± 0.03 m/s to keep the random noise down. The instrument measures over a small sampling volume of less than 0.25 cm^3 at a point 5 cm away from the sensors, here at a sampling rate of 10 Hz.

Figures 1 and 2 show vertical velocity distributions at the centreline of the flume for $Q = 1.6$ l/s and $Q = 7.2$ l/s, respectively. Figure 1 also displays the theoretical laminar velocity parabola, the outcome from a least-squares fit and one more parabolic fit to the data with the additional condition of the velocity maximum occurring at the free surface. As can be seen from the figure, the measured velocity distribution is distinctly flatter than its theoretical fully laminar counterpart. This indicates a transitional regime, which agrees with the Reynolds number being right in the interval between 500 and 2000. From the viewpoint of the criteria presented in the previous section, the flatter velocity distribution results in lower values of $(\partial u/\partial z)^2$ as compared to those derived from laminar theory. The criterion, Eq. (14), therefore cannot be expected to be "on the safe side" in this case. The same, of course, holds true for the less stringent conditions Eqs. (18) and (19), but even more so.

Figure 2 shows the measured velocites for the turbulent case of $Q = 7.2$ l/s, together with the hydraulically smooth log-law velocity distribution ($u^* = 1.446$ mm/s). Fitting the hydraulically rough version to the data had shown the criterion $u^* k_s/\nu < 5$ to apply, which agrees with the fact that the bottom of the flume indeed had a smooth and even surface

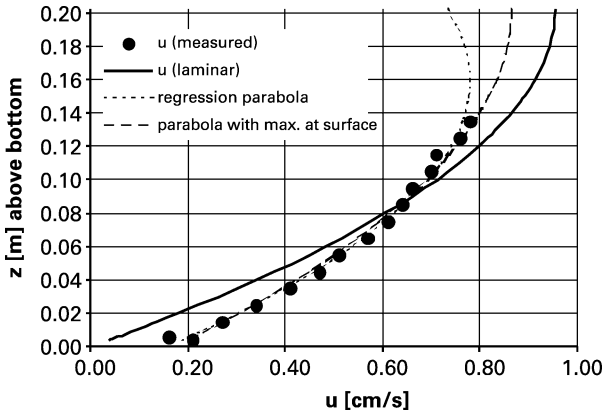

Figure 1 Vertical velocity profile for $Q = 1.6$ l/s

(concrete, cement-coated). No wake term was used in this context, as an extensive search involving more than 4000,000 pairs of u^* and Π had identified the best fit for zero wake strength (in agreement with Nezu and Rodi (1986)).

Table 1 gives a survey of the characteristic data of the tracer experiments. For one of the runs potassium bromide was used, while in all others the tracer was sodium chloride. Breakthrough curves were measured by electric conductivity probes, the readings of which were converted to chloride or bromide concentrations in the laboratory. This technique was chosen as it permits continuous records to be obtained, and errors due to external sources of electrolytes can be ruled out in the laboratory. The chloride/bromide versus conductivity relationships proved quite stable, with very little scatter.

The values of vertically mixed, initial concentration C_{init} listed in Table 1 were computed from Eq. (4) and measures were taken to ensure that full initial vertical mixing did actually take place (injection into the inflow weir overfall). The aspect ratio B/h of $1.5\,\text{m}/0.2\,\text{m} = 7.5 > 5$ was sufficient for the development of an essentially two-dimensional flow near the centreline of the flume, not influenced by the side walls (Nezu *et al.* 1993). Additionally, the adequacy of the aspect ratio used here was confirmed by experiments in the near-laminar transitional regime (Stephan 2001). Discharge per unit width at the centreline of the flume was estimated from Q/B and then corrected for transverse non-uniformity. This correction was based partly on velocity measurements (cases of 20 cm water depth) and partly on depth integrals of the laminar velocity field as given by Wagner (1969) for laminar

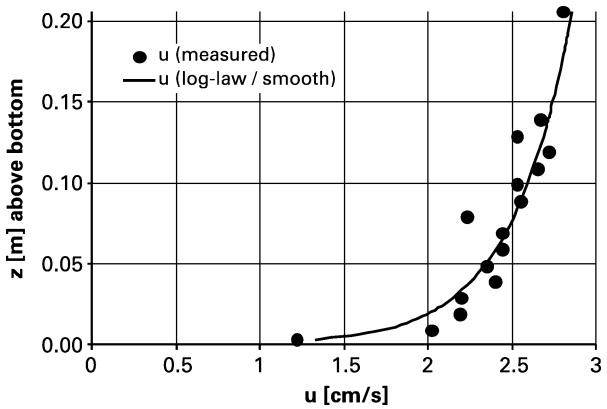

Figure 2 Vertical velocity profile for $Q = 7.2$ l/s

Table 1 Characteristic data of pulse injections

Run no. [−]	Salt [-]	Temp. [°C]	Q [l/s]	h [cm]	q/(Q/B) [-]	q [m^2/s]	Re [-]	Re (centreline) [−]	M_0 (salt) [g]	Δt [min]	C_{init} [mg/l]
1	NaCl	15.6	1.6	20.0	1.18	0.00126	946	1116	5562.5	8.5	6816.8
2	NaCl	18.1	1.6	20.0	1.18	0.00126	1007	1188	76.7	10	79.9
3	KBr	18.0	1.6	20.0	1.18	0.00126	1005	1185	669.0	10	696.9
4	NaCl	21.5	1.6	20.2	1.18	0.00126	1093	1289	13.7	10	14.3
5	NaCl	21.5	1.6	20.2	1.18	0.00126	1093	1289	27.4	10	28.5
6	NaCl	21.0	7.2	20.2	1.04	0.00499	4859	5054	3941.0	10	912.3
7	NaCl	21.0	1.6	20.0	1.18	0.00126	1080	1274	62.3	10	64.9
8	NaCl	21.6	7.2	20.2	1.04	0.00499	4928	5126	585.5	10	135.5
9	NaCl	16.7	1.4	11.2	1.10	0.00103	851	939	52.9	10	61.5
10	NaCl	16.9	1.2	10.6	1.10	0.00088	733	805	33.8	10	45.7
11	NaCl	17.0	1.2	10.6	1.10	0.00088	735	807	29.4	10	39.7
12	NaCl	17.2	7.2	10.3	1.04	0.00499	4431	4609	260.4	4	150.0
13	NaCl	17.2	7.2	10.3	1.04	0.00499	4431	4609	312.5	4	180.0
14	NaCl	17.2	7.2	10.3	1.04	0.00499	4431	4609	434.0	4	250.0

flows in rectangular open channels. The correction factors applied are listed in Table 1 in a column between Q and q.

For the first run listed in Table 1, the presence of density stratification was judged from vertical concentration profiles (see Figure 3, $x = 34.15$ m downstream of the injection, recorded some 10 h after the tracer release). For all others, four electric conductivity meters were mounted at $x = 34.15$ m (centreline) at fixed distances (for $h \approx 20$ cm: $z = 1.5$ cm, 5 cm, 10 cm and 15 cm from the flume bottom, while for $h \approx 10$ cm: $z = 1.5$ cm, 4 cm, 6.5 cm and 9 cm). An example of the breakthrough curves recorded at $x = 34.15$ m is shown in Figure 4.

For instantaneous slug releases or short pulse injections density effects cannot be inferred from vertically non-uniform concentration distributions alone, as such non-uniformities will also appear due to shear flow dispersion in cases of neutrally buoyant solute transport. However, the zeroth moments (area under the curve) of concentration versus time distributions will be equal in well-mixed conditions (Airey *et al.* 1984), a fact that forms the basis of most discharge measurements by the tracer dilution technique.

Table 2 summarizes the normalized zeroth moments of all pulse injection experiments with recorded breakthrough curves at the four different depths given above. Normalization was done to facilitate comparison of uniformness or non-uniformness among the various experiments. The "areas" under the breakthrough curves of each run were scaled such that the average of the values at the four respective depths becomes unity.

In almost half of the cases, the values listed in Table 2 indicate strong density effects. This is clearly so for runs no. 2 and 3, whereas run 4 might be termed a borderline case, with

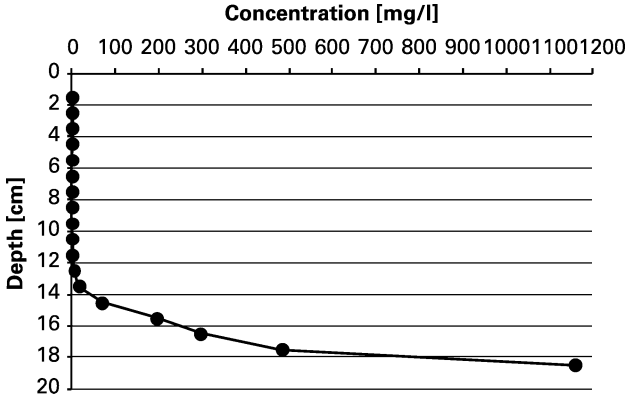

Figure 3 Chloride concentrations versus depth, measured at $x = 34.15$, run no. 1

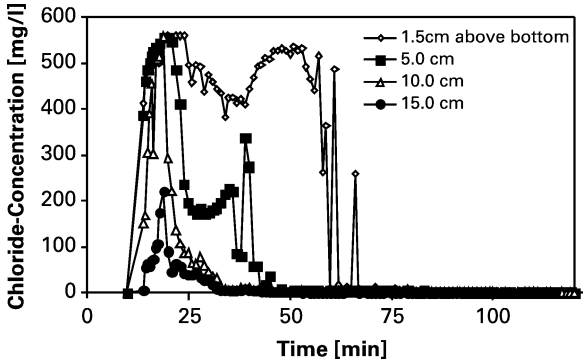

Figure 4 Chloride breakthrough curves of run 6, showing clear signs of density stratification

Table 2 Normalized zeroth moments of breakthrough curves at different depths above the bottom

Run no.	Salt	1.5 cm	5 cm	10 cm	15 cm
2	NaCl	2.65	0.87	0.27	0.22
3	KBr	3.57	0.37	0.05	0.02
4	NaCl	1.27	0.79	0.91	1.04
5	NaCl	2.40	0.94	0.34	0.32
6	NaCl	2.47	0.96	0.44	0.13
7	NaCl	2.65	0.99	0.28	0.09
8	NaCl	1.60	1.10	0.83	0.47
Run no.	**Salt**	**1.5 cm**	**4 cm**	**6.5 cm**	**9 cm**
9	NaCl	1.25	1.05	0.92	0.77
10	NaCl	1.47	0.71	0.99	0.83
11	NaCl	1.22	0.94	0.86	0.98
12	NaCl	1.10	1.05	1.04	0.81
13	NaCl	1.10	1.08	1.03	0.79
14	NaCl	1.19	1.16	1.08	0.58

the normalized zeroth moments in a range of $\pm 30\%$ of unity, showing no steady trend with depth. The outcome from run 5, in contrast, again indicates the presence of density stratification, and so do runs 6 and 7 (Table 2). In comparison, the trend in the zeroth moments of the breakthrough curves from run 8 might be termed moderate, though the presence of density effects is still quite pronounced.

Runs 9–11 are close to borderline cases with only weak density effects. In these experiments, the water depth was reduced by 50% compared to the runs described above, so as to allow experimentation at a Reynolds number distinctly below 1000 without arriving at C_{max} values below the detection limit of the conductivity meters.

Runs 12–14 with $Q = 7.2$ l/s and $h = 10.3$ cm are within the turbulent regime, with no stratification observed for initial salt concentrations of 150 mg/l and 180 mg/l, respectively. Run 14 ($C_{init} = 250$ mg/l) shows the first signs of slight density effects.

Table 3 now compares the actual concentrations after initial vertical mixing, C_{init}, to the maximum values permitted by the criteria developed in the previous section of this paper, Eqs. (14), (18), (19) and (24), respectively.

To begin with, it can be noted that Eq. (18) and its first-order approximation, Eq.(19), produce the same results (at least to the first digit in mg/l), so that no further distinction will be made between these two formulae.

In a number of cases the concentration actually used is much larger than the computed limit and the predicted stratification was observed very clearly. As described above on the basis of zeroth moments, the pulse injection of run 4 might be termed a borderline case. The criterion, Eq. (14), is fulfilled, so that one might have expected less density effect than was actually observed. This could be explained by an examination of the velocity profile, Figure 1: as remarked before, the deviation of the velocity distribution with depth from the one underlying Eq. (14), i.e. the theoretical laminar one, causes the formula to overpredict C_{max} by the amount of approximately 21%. Correcting for that, one obtains a limit of 12.1 mg/l instead of 14.6 mg/l, now below the actual value of $C_{init} = 14.3$ mg/l, which indicates a situation between borderline and weak density stratification. From that, it becomes clear that (for $Ri_{b,max} = 0.25$) the performance of Eqs. (18) and (19), respectively, is inferior to that of Eq. (14), and that a choice of maximum Richardson number in excess of the value of 0.25 recommended in the literature (and underlying the above criteria) would not be supported by the data. This conclusion is confirmed by the results from runs 9 and 10, where Eq. (14) clearly outperforms Eqs. (18) and (19), and from run 11, which indicates only

Table 3 Comparison of predicted and observed density effects

Run no. [–]	C_{init} [mg/l]	C_{max} {Eq. (14)} [mg/l]	C_{max} {Eq. (18)} [mg/l]	C_{max} {Eq. (19)} [mg/l]	C_{max} {Eq. (24)} [mg/l]	stratification pred. {Eqs. (14),(24)}	stratification pred. {Eqs. (18),(19)}	stratification observed
1	6816.8	14.7	19.6	19.6	–	yes	yes	yes
2	79.9	14.8	19.8	19.8	–	yes	yes	yes
3	696.9	14.8	19.8	19.8	–	yes	yes	yes
4	14.3	14.6	19.5	19.5	–	borderline	no	borderline/weak
5	28.5	14.6	19.5	19.5	–	yes	yes	yes
6	912.3	–	–	–	136.0	yes	–	yes
7	64.9	14.9	19.9	19.9	–	yes	yes	yes
8	135.5	–	–	–	136.7	borderline	–	moderate
9	61.5	56.4	75.2	75.2	–	borderline	no	borderline
10	45.7	48.4	64.5	64.5	–	borderline	no	weak
11	39.7	48.4	64.5	64.5	–	no/borderline	no	borderline/no
12	150.0	–	–	–	1000.0	no	–	no
13	180.0	–	–	–	1000.0	no	–	no
14	250.0	–	–	–	1000.0	no	–	no/borderline

slightly stronger density effects than would be expected from Eq. (14) – probably due to deviations from the fully laminar velocity profile. The stratification observed in the course of run 11 is again considerably stronger than that predicted from Eqs. (18) and (19).

From Table 3 one can see that the criterion for turbulent conditions, Eq. (24), somewhat overpredicted C_{max} for run 8 (with a borderline case expected and a moderate stratification actually observed) and underpredicted for run 14 (in the case of runs 12 and 13 no stratification was expected due to Eq. (24), and none was observed). Detailled examination of the breakthrough curves from run 14 revealed that only one of these curves (the uppermost) differed notably from the rest, whereas the other three nearly coincided, thereby indicating (partly) well-mixed conditions. Thus, a further increase in salt concentration would very probably not have resulted in the immediate development of strong stratification, so that Eq. (24) is likely to have given the correct order of magnitude also in this case. However, it is clear that continued research extending the database on salinity-induced density stratification in turbulent flows at comparatively low Reynolds numbers will certainly be helpful.

Conclusion

Criteria to judge the importance of density effects in the course of salt tracer experiments have been developed, explicitly addressing the range of Reynolds numbers typical of constructed wetland ponds. It has been found that stringent limits to the salt injection mass exist, particularly in the laminar and transitional flow regimes. As the signal due to the injection must remain detectable at the outlet of the wetland pond, the mass injected cannot be lowered arbitrarily so that the use of salt tracers may become impractical in cases of particularly low Reynolds number flows.

Acknowledgement

The research reported here was partly funded by the European Commission under contract no EVK1-CT-2000-00065 (PRIMROSE). This support is gratefully acknowledged.

References

Airey, P.L., Calf, G.E., Davison, A. and Morley, A.W. (1984). An evaluation of tracer dilution techniques for gauging of rivers in flood. *J. Hydrol.*, **74**, 105–118.

Boehrer, B., Ilmberger, J. and Münnich, K.O. (2000). Vertical structure of currents in western Lake Constance. *J. Geophys. Res.*, **105**(C12), 28823–28835.

Crowley, W.P. (1968). A global numerical ocean model: part1. *J. Comput. Phys.*, **3**, 111–147.

Graf, W.H. and Cellino, M. (2002). *J. Hydraul. Res.*, **40**(4), 435–447.

Hammer, D.E. and Kadlec, R.H. (1986). A model for wetland surface water dynamics. *Wat. Resources*, **22**(13), 1951–1958.

Henderson, F.M. (1966). *Open Channel Flow*. Macmillan, New York, p. 95.

Howard, L.N. (1962). Note on a paper of John W. Miles. *J. Fluid Mech.*, **10**, 509.

Kadlec, R.H. and Knight, R.L. (1996). *Treatment Wetlands*. CRC Press, Boca Raton, FL, pp. 618–619.

Koskiaho, J. (2003). Flow velocity retardation and sediment retention in two constructed wetland-ponds. *Ecol. Engng.*, **19**(5), 325–337.

Miles, J.W. (1962). On the stability of heterogeneous shear flows. *J. Fluid Mech.*, **10**, 496–508.

Nezu, I. and Rodi, W. (1986). Open channel flow measurements with a Laser Doppler Anemometer. *ASCE J. Hydraul. Engng.*, **112**(5), 335–355.

Nezu, I., Tominaga, A. and Nakagawa, H. (1993). Field measurements of secondary currents in straight rivers. *ASCE J. Hydraul. Engng.*, **119**(5), 598–614.

Persson, J., Somes, N.L.G. and Wong, T.H.F. (1999). Hydraulics effficiency of constructed wetlands and ponds. *Wat. Sci. Technol.*, **40**(3), 291–300.

Rutherford, J.C. (1994). *River Mixing*. John Wiley and Sons, Chichester, pp. 86–93.

Sabir, I.H., Haldorsen, S., Torgersen, J., Aleström, P., Gaut, S., Colleuille, H., Pedersen, T.S. and Kitterød, N.-O. (2000) Synthetic DNA tracers: examples of their application in water related studies. *TraM'2000 Conf. Proc., Liege*. IAHS Publ. No. 262, pp. 159–165.

Stephan, U. (2001). Personal communication.

Wagner, H. (1969). Theoretische Untersuchungen der Abflußcharakteristik in beliebig gestalteten, offenen Rechteckprofilen (Theoretical study of free surface flows in rectangular open channels of arbitrary aspect ratio). *Habilitationsschrift* Technische Universität Dresden (in German).

Woolhiser, D.A. (1975). Simulation of unsteady overland flow. In: *Unsteady Flow in Open Channels*. (Eds. K. Mahmood and V. Yevjevich). Water Resources Publications, Fort Collins, CO, vol 2, pp. 485–508.